EMAS Engineering Modelling, Analysis & Simulation THE NAFEMS JOURNAL

NAFEMS

Vol. 4, Issue 1, 2027

Analysis Driven Innovation of a Fusion Power Plant Plasma Facing Component

Tom Deighan[1]

UKAEA (United Kingdom Atomic Energy Authority), Culham Campus, Abingdon, OX14 3DB, UK

Abstract

The STEP (Spherical Tokamak for Energy Production) Programme targets delivery of a UK prototype fusion energy power plant by 2040, to demonstrate a path to commercial viability of fusion power. A critical aspect to designing a fusion power plant is being able to extract useful energy out within the operating constraints of the plasma facing components, which must handle high heat fluxes over a sustained period. Increasing the heat loading capacity of these components widens the operating envelope for the plasma and ultimately enables high power outputs to be achieved. Key to enabling delivery of the STEP program, and ultimate realisation of commercially viable fusion power, will be the concurrent consideration of multiple component designs, including continued creation and exploration of novel concepts using appropriate analysis and simulation techniques to explore their feasibility efficiently and effectively. This paper presents innovative plasma facing component design concepts, providing an optimisation of the heat flux distribution and heat transfer, to increase the heat loading capacity within structural and thermal operating constraints, and in consideration of broader design objectives. Efficient simulation and analytical methods are developed and applied to optimise aspects of the design and explore the feasibility of solutions effectively, providing assessments of the thermal and structural performance in comparison to a more conventional design. Specifically, the analysis is used to quantify how the increased design freedom from optimisation can be exploited, such as reduced material quantities, increased heat flux operating window or increased component lifetime. The paper also demonstrates the value in using an analytical approach to aspects of design innovation to readily evaluate the feasibility and potential for novel design concepts. Finally, the paper outlines the main design challenges and further research and development work needed to explore the potential of the design concepts further, requiring expertise and involvement from wider industry.

Keywords

Design Optimisation, Fusion Power, Plasma Facing Component

© (2026) The Authors. Published by NAFEMS Ltd.

This work is licensed under a Creative Commons Attribution-NonCommercial-NoDerivatives 4.0 International License.

Peer-review under responsibility of the NAFEMS EMAS Editorial Team.



1 Introduction

One of the current favoured Plasma facing component designs to handle high heat fluxes is the Monoblock design shown in Figure 1. Under normal steady state operation (plasma flat top) the highest loads will occur on the divertor (exhaust) with components proposed to handle

[1]Corresponding author.
E-mail address: tom.deighan@ukaea.uk (T. Deighan)
https://doi.org/10.59972/ry897brj

heat fluxes of around 10 MW/m^2 and very short duration extremes, potentially up to orders of 1 GW/m^2, during transient events resulting from plasma instabilities and disruptions.

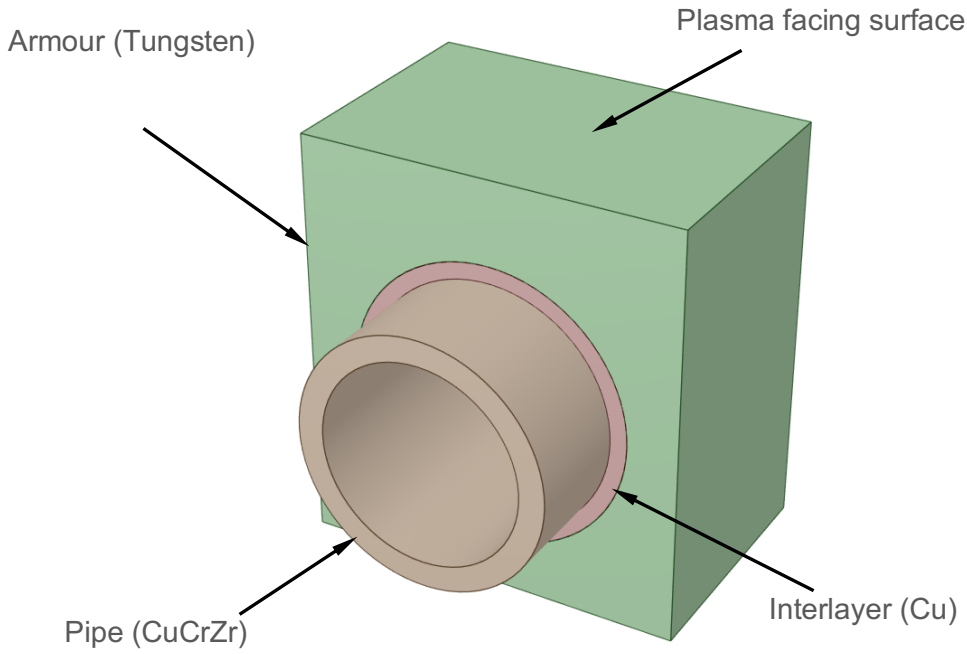


Figure 1. Monoblock plasma facing component design.

Under the extreme loads from these discrete events, material melting and vaporisation of the surface and sub-surface will likely occur, with additional secondary effects [1], [2]. Understanding and simulating the behaviour under these events is still uncertain and the subject of research. Ensuring adequate lifetime of the components will be a balance between mitigating actions and control to limit or prevent these events from occurring, and from improved understanding and confidence in simulation to ensure rates of material loss and surface modifications are within acceptable limits. Adequately handling the steady state heat fluxes remains a significant challenge however with the conventional designs shown in Figure 1 having some fundamental limitations, discussed further in Section 2.

Various novel concepts have and are being developed to address these challenges along with other challenges associated with the effects of the neutron irradiation environment on the component materials. These include modifications to the conventional monoblock through use of advanced materials and additively manufactured graded materials [3], cooling tube inserts to enhance the heat transfer [4] and also fundamentally different concepts such as use of liquid metal armours [5]. Each of these designs offer potential advantages, some combinable into an overall solution, whilst also introducing new challenges.

This paper focuses on the use of simplified analysis to inform novel optimisations on the interfacing structure between the cooling pipe and plasma to address the limitations on thermal-structural performance. The potential concepts and proposed technologies outlined in the references in the previous paragraph are excluded from any developments here, maintaining the same materials and cooling tube arrangement. The optimisations are based on allowing the following design freedoms:

1. Large scale topography (shaping) of the plasma facing surface (Section 3),
2. Topology of the armour structure (Section 0),
3. Motion of structure (Section 5).

This work relates to patent application GB2602699.7. Additionally, the paper demonstrates the benefit of deploying appropriately simplified analytical techniques, providing the freedom to investigate and develop novel concepts rapidly, for which the use of more advanced numerical methods can often be constraining

2 Reference Baseline

A reference baseline thermal-structural FE model is shown in Figure 2, with a nominal 10 MW/m2 heat flux and coolant HTC assuming water cooling without nucleate boiling. The structural model is identical, with temperature loads applied only. The symmetry planes are adiabatic with zero normal displacement and zero shear.

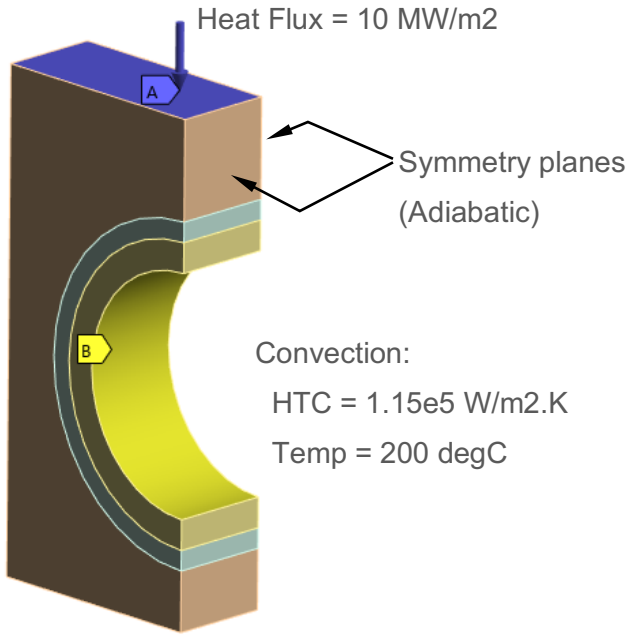


Figure 2. Reference baseline thermal model.

2.1 Materials

The precise material properties and models used do not strongly influence the findings from this work, however the properties are summarised in the tables below for reference.

Table 1. Basic thermal structural material properties.

Property	Tungsten	Copper	CuCrZr
Density (kg/m3)	19250	8960	8900
Elastic Modulus (GPa)	280	110	120
Poisson Ratio	0.28	0.33	0.33
Thermal conductivity (W/m.K)	152 at 20 °C 104 at 600 °C 95 at 1000 °C	320 at 20 °C 345 at 400 °C	400 at 20 °C 375 at 400 °C

Table 2. Material plasticity.

Stress (MPa) / Plastic Strain	Copper		CuCrZr	
	20 °C	400 °C	20 °C	400 °C
	Combined iso/kinematic		Perfectly plastic	
0.002	64	33	290	210
0.01	81	44		
0.1	117	69		

2.2 Assumptions

The following assumptions are made for the reference baseline analysis and for the proceeding topology optimisation.

- Surface heat flux only, neglecting volumetric heating from neutron flux.
  For the highest loaded regions of the divertor the thermal response is dominated by the surface heat load.
- Edge loading (due to gap between blocks) is neglected.
  In practice for this design some profiling will be applied to prevent this.
- Manufacturing residual stress is neglected.
  This is an area of large uncertainty and although it will have a major impact on ultimate durability it is unlikely to change the results of topology studies (at least without including simulation of the manufacturing process itself) or of any relative comparisons to the baseline.
- Coolant pressure load is neglected.
  Effect in stresses are small compared to thermal loading.
- Steady state operations (plasma flat top) are considered only.
  Under these conditions structural response is dominated by thermal loads. Ultimately any final design must also consider other load cases including transient events such as disruptions, where short duration higher peaks in heat flux and mechanical loading can occur. There is considerable uncertainty on the characteristics and occurrence of these load cases and has been excluded from this work for both the reference design and proposed designs.

2.3 Results

Results from the baseline analysis are shown in Figure 7.a and Figure 8.a which both provide a reference for assessing potential design alternatives and also highlight the limitations referred to previously. These include:

1. The heat flux is focused on the plasma facing surface and conducted to a coolant channel with the material on the opposite side of the channel unutilised. This unutilised material remains at a much lower temperature and acts to constrain the expansion of the upper part of the block, inducing stresses in the structure. Temperatures are readily calculable from an equivalent lumped mass model consisting only of the upper material - also demonstrating the lack of usefulness of the “wasted material”. The stress value indicated by * in Figure 8.a indicate that resulting from thermal gradients in the armour alone, neglecting differential expansion of the pipe and interlayer.
2. Tungsten is a favoured material for the plasma facing surface for its high melting point amongst a number of reasons, whilst CuCrZr is favoured for the piping. This creates a large mismatch in thermal expansion coefficient across the joint leading to additional induced stresses in the Tungsten (see Figure 8.a). A pure copper interlayer acts to

both improve the joining of these components and to help alleviate this mismatch through significant plastic deformation. This itself creates a potential lifetime limitation under repeated thermal cycles.

Achieving commercial viability of fusion will rely on minimising manufacturing costs where possible and having this amount of "unutilised" Tungsten is a significant cost for no return. Eliminating this unutilised material will also help to minimise future activated waste streams. The main motivation of the work in this paper is to search for potential designs which either eliminate the unutilised material or retain it to provide value in enabling higher heat fluxes or increased lifetime.

3 Plasma Facing Surface Topography

The shape of the plasma facing surface of a tokamak fusion power plant is designed based on the operating shape of the plasma. Monoblock components like that in Figure 1 are arranged to create the shape of the plasma facing surface. Looking locally at specific monoblocks the plasma intercepts the flat plane of the surface at an angle of incidence, reduction of which spreads the heat load over a larger surface and reduces the heat flux magnitude. Minor profiling of the surface is likely needed to eliminate loading of the edges due to the required assembled gap between blocks and accounting for manufacturing and assembly tolerances [6]. Large scale shaping of the surface however is proposed here, along with other modifications, to spread the heat loads further and improve the overall heat transfer to the coolant.

A fully cylindrical profile is considered as shown in Figure 3. Under this geometry the ratio of the heat flux relative to that on a flat reference plane (as per the reference monoblock design) can be calculated as a function of the circumferential position around the cylinder surface, dependant on the orientation angles ψ and β as,

$$qr(\theta) = cos(\theta) + \frac{sin(\theta)}{tan(\psi)} \cdot cos(\beta) \qquad \text{for} \quad \theta_1 \leq \theta \leq \theta_2 \qquad (1)$$

where qr = heat flux ratio (ratio of heat flux to that on the “flat” reference plane), θ = angular position around of cylinder, ψ = plasma incident angle relative to “flat” reference plane, β = azimuth cylinder orientation angle and θ_1, θ_2 = angular extents.

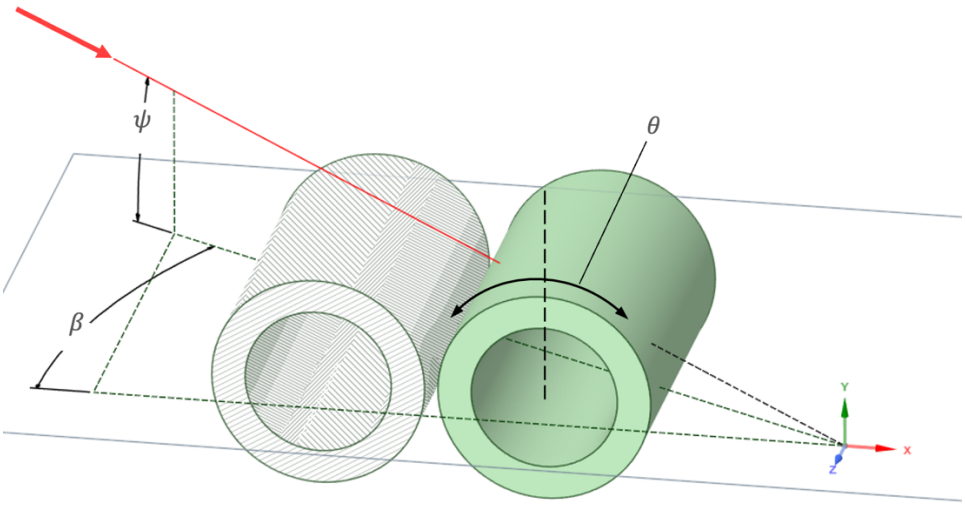


Figure 3. Orientation of cylindrical surface to plasma and reference plane.

The angular extents of the loading θ_1, θ_2 are a function of the orientation angles and limited by shadowing of the adjacent component (cross hatching in Figure 3). As with the conventional monoblock design a gap between the components is needed to allow for manufacturing and assembly tolerances and thermal expansion. For a given nominal incident angle ψ, the azimuth orientation β is limited to prevent shine-through of the plasma between the gaps. The heat flux ratio is plotted in Figure 4 for specific reference incident angles and azimuth orientations. With $\beta = 0$ the angular extent is limited for shallow incident angles and the peak heat flux increased compared with a flat plane where the incident particles impinge closer to the surface normal. Although this obviously has no benefit for a static component, this is revisited in Section 5. As β is increased the heat is spread over an increasing extent with the ratio of loaded surface perimeter to diameter shown in Figure 5, compared to a value of 1.0 for the reference baseline monoblock. The perimeter increase tends towards 57% $(\pi/2 - 1)$ as β tends to 90deg. Although the ratio is seen to be slightly larger than unity (limited by $\beta <$ 90deg to avoid shine-through), and in practice some margin over $\beta = \beta_{max}$ would be needed to ensure the design is robust to plasma variations, there should be a potential benefit in the fact that the heat load is spread over a large area. This is assessed further with regards to topology optimisation of the structure in Section 4.

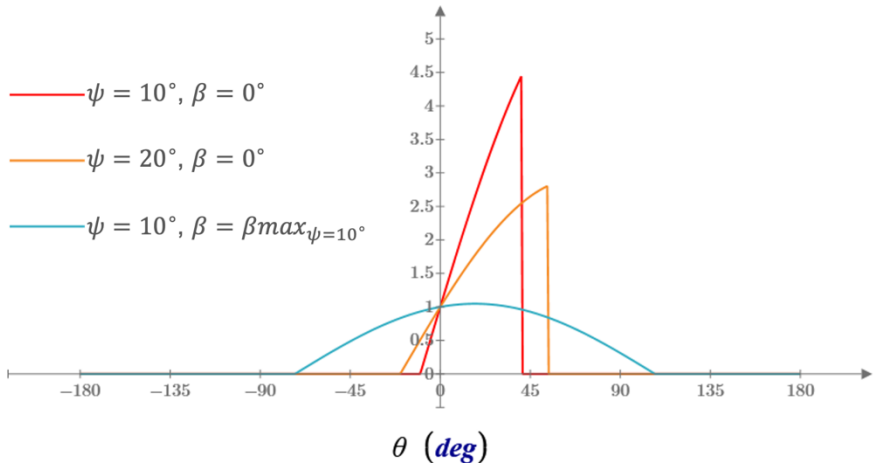


Figure 4. Heat flux ratio (compared to flat reference plane) for varying orientation angles.

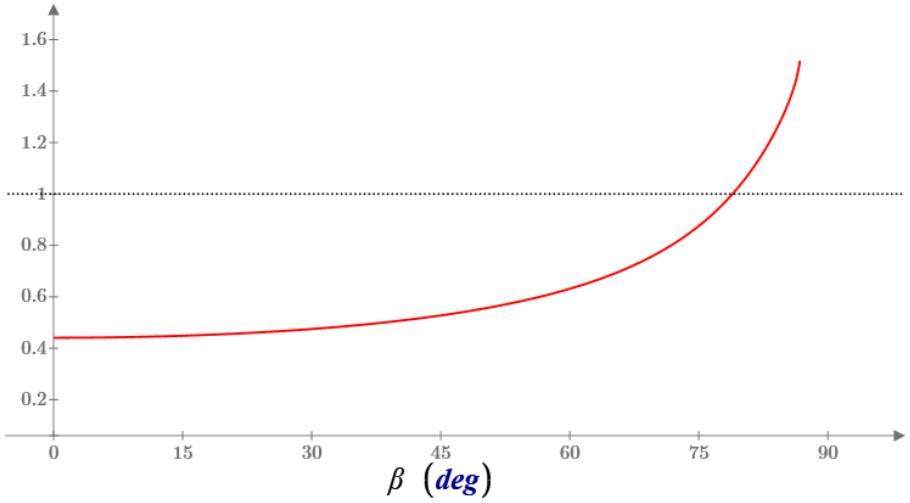


Figure 5. Heat loading perimeter over cylinder relative to baseline flat monoblock as a function of orientation angle.

4 Topology Optimisation

Topology optimisation can be a highly valuable technique to provide guidance on the fundamental topological design of structures during early concept development. Although used widely across various industry sectors, the technique is under used in the fusion sector, where it could have a significant influence on informing novel designs, especially to help keep material use and manufacturing costs down.

Considering thermal performance, a topologically optimised shape for the armour is relatively self-evident from the temperatures shown in Figure 7.a, where, as discussed in Section 2, this material is not utilised and in fact acting to increase the component stresses. Considering durability, an optimum topology is maybe less obvious, where a design could be envisaged which forces heat to be transferred further around the cooling pipe helping to even out the temperature distribution. In either case performing a simple FE topology optimisation can help confirm or inform an optimised design and provide a determinate bound to the modifications.

Performing topology optimisation in widely available FEA solvers normally requires a linear model in most respects. The model in question contains two predominant areas of non-linearity, temperature dependant material properties and localised plastic deformation. Additionally, where nucleate boiling might occur this introduces non-linearity to the heat transfer coefficient of the coolant. Although linearising the model to remove these has a significant influence on the results it does not prevent the use for topology optimisation as a tool to inform potential solutions. The workflow used is shown in Figure 6.

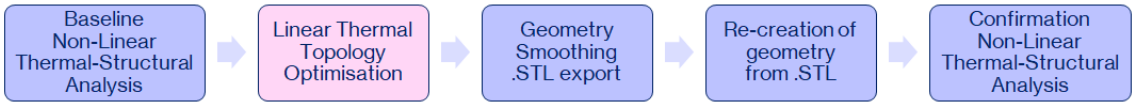


Figure 6. Topology optimisation workflow.

The topology optimisation was performed in ANSYS Mechanical using both the SIMP based density method [7] (with a penalisation factor of 3) and the level set method [8]. Both gave almost identical results and therefore only the density method results are presented here. The Tungsten armour and interlayer were set as designable and the copper pipe excluded from the optimisation. The optimisation objective was set to minimise the thermal compliance (i.e. maximise the conduction through the structure) with a constraint to retain 50% of the designable volume.

A topology optimisation was run on the baseline reference design and on a variant with an optimised surface topography and incident plasma orientation, as discussed in Section 3. Overall, the following design variants are compared:

A Baseline reference design

B Topology optimised armour structure

C Cylindrical surface topography with optimised incident plasma orientation ($\beta = 90\mathrm{deg}$, neglecting shine-through)

D As c) with topology optimised armour structure

Thermal results and structural results are shown for each of the design variants in Figure 7 and Figure 8, a) to d) respectively. Figure 7 also shows the corresponding percentage mass reduction in the Tungsten armour.

Considering topology optimisation of the baseline design, B, the results show that close to 50% of the Tungsten armour can be removed whilst maintaining similar peak temperatures, similar durability of the armour and improved durability of the pipe and interlayer. The removed

material follows intuitively what was expected from examining the performance of the baseline design.

Although having some armour material wrapping around the pipe acts as a fail-safe to retain the armour in case of a failure of the brazed joint, in practice a failure of this magnitude of the brazed joint would regardless prevent any operations and require replacement. In practice some additional material would be needed to facilitate mounting the component to the supporting structure and transfer structural loads. As with the baseline design however this mounting structure will not be necessary on every consecutive block and with the optimum design likely to only require a fraction of the original material. Therefore, although some additional material will be required this will only be a fraction of the original with the optimum mounting topology to be assessed following better understanding and inclusion of the structural loading.

Utilising a design with a cylindrical surface C, immediately provides a 16% mass reduction and with an optimised orientation (as outlined in Section 3) reduces temperatures compared to the baseline, due to both the spread in heat load and the reducing the average conductance path to the coolant.

Combining both within design D provides the largest mass reduction of almost 60%, reduced temperatures, improved pipe and interlayer durability and a tolerable 13% increase in peak stress in the armour. With this optimised surface shape, the results show material retained to valuable use further around the cooling pipe.

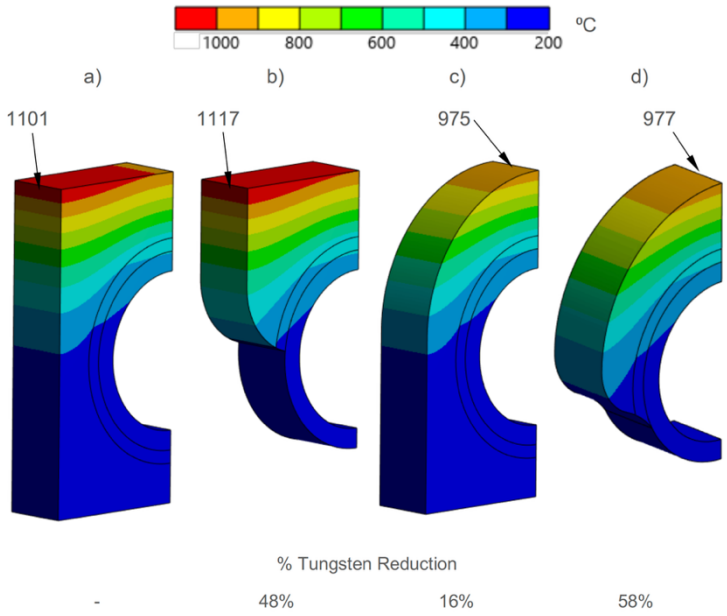


Figure 7. Temperatures and corresponding mass reduction for design variants.

Although the results presented make certain assumptions, such as neglecting structural loads and neglecting robustness margin when maximising favourable orientations, they identify potential solution directions and bound the possible savings in material volumes and improvements in durability. Subject to further analysis, considering structural loading and other effects, the results show potential for significant saving in the volume of Tungsten material required and therefore component costs.

Potential designs have been investigated in the past to improve durability by increasing the thermal resistance to the coolant in the centre region, to force heat transfer further around the coolant pipe and in doing so also create some structural compliance between the pipe and armour [9]. To investigate possible design solutions in this area the topology optimisation was

also run considering the durability response within the optimisation, with the objective changed to minimise the stresses rather than thermal conductance. The results gave an almost identical solution to the thermal only topology optimisation.

Although aspects of the optimisations shown here, and designs such as that in [9], enable some improvement in material utilisation, reducing temperatures and improving aspects of durability, the ability to realise this benefit for significant increase in operational lifetime or increased heat load capacity, is fundamentally limited by the unidirectional heat flow. Realisation of any benefit is dependent on gaining further knowledge of material behaviour and validation of the critical durability limitations.

The following section aims to address this limitation by utilisation motion of the component to transform the unidirectionally localised static heat load into a distributed transient time-varying load.

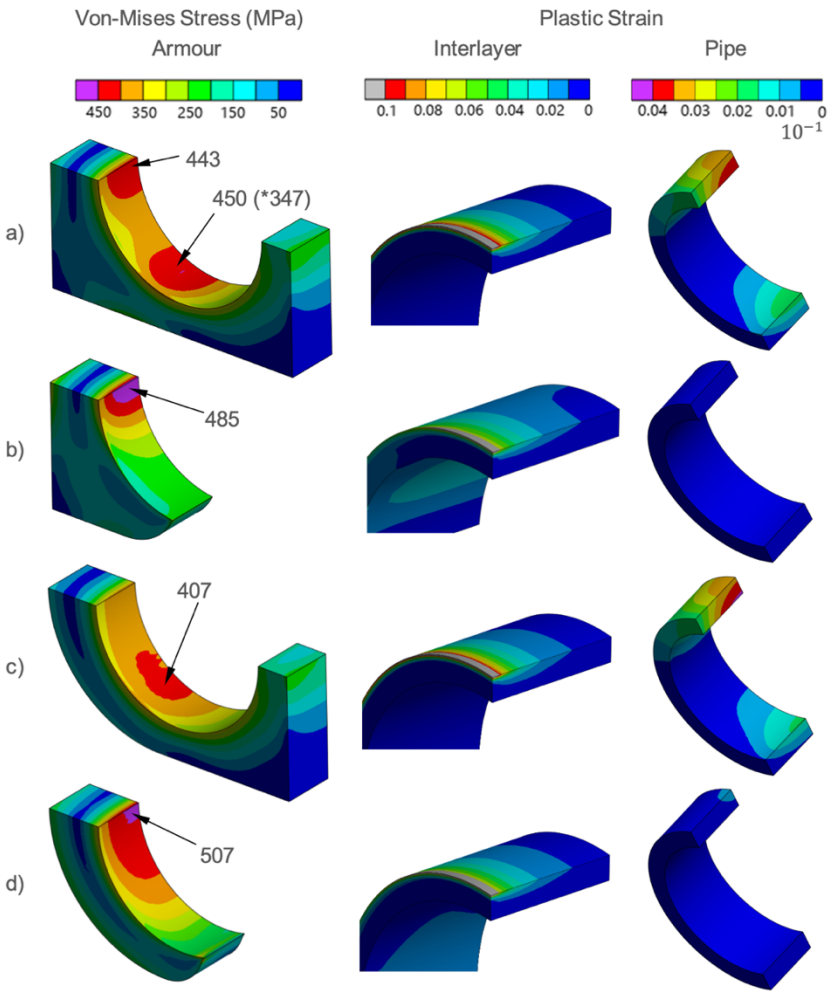


Figure 8. Structural results for design variants (* shows stress in armour for baseline if pipe and interlayer are excluded from the structural model).

5 Rotating Surface

The concept outlined in this section has two principal aspects as outlined below.

3. Rotating surface: Due to the rotation of the cylinder, any point on the surface now sees a periodic time varying heat flux, the average of which over one rotation being reduced

compared to that on the plane fixed surface of the Monoblock. The periodic fluctuations in temperature about the mean are limited in amplitude and depth below the surface by the speed of rotation.

4. Bearing: The bearing provides a means to allow the plasma facing cylinder to rotate relative to the pipe whilst also providing:
   - Thermal conductance for the average heat flow to the pipe and coolant
   - A level of structural decoupling between the cylinder and pipe removing the sudden thermal expansion mismatch
   - Enabling greater control and reduced uncertainty of the "as manufactured" stress state of the component

Supporting analysis to assess the viability of the concept is outlined in the following sections.

5.1 Concept Fundamentals

By rotation of the cylinder the heat loading is transformed into a periodic time-varying load which for a point on the surface is given by Equation 1 and as plotted in Figure 4 with θ replaced by ωt, where ω is the speed of rotation. This can be decomposed into a mean (time averaged) heat flux and a Fourier series.

The total heat input must obviously remain the same with the time averaged heat flux ratio therefore being a simple function of the total loaded area relative to the projected area in the reference plane. This is given by,

$$qr0 = \frac{1}{2\pi} \cdot \frac{2r + \delta}{r} \tag{2}$$

with $\delta =$ gap between components and $r =$ radius of cylinder. This can also be confirmed by integration of curves in Figure 4.

As the gap between the cylinder is small relative to the cylinder diameter ($\delta \ll r$), in the limit, the heat flux ratio is equal to a constant $1 / \pi = 0.318$, meaning the mean heat flux which must be conducted through the structure and into the coolant is reduced to ≈32% of that from a fixed surface.

The periodic time varying load will cause near surface fluctuations in component temperature but will not affect the net thermal load into the coolant. The frequency of fluctuation, determined by the rotational speed of the cylinder, will affect the depth of penetration and magnitude of these temperature fluctuations. Temperature fluctuations are calculated by solving the 1D (radial) transient heat PDE with boundary conditions shown below.

$$\rho . c_p \frac{\partial u}{\partial t}(x,t) = k \frac{\partial^2 u}{\partial x^2}(x,t)$$

$$u \to 0, x \to \infty$$

$$q(0,t) = -k \frac{\partial u}{\partial x}(0,t) = Q0 \cdot qr(\omega t)$$

where $Q0 =$ heat flux on “flat” reference plane, $k =$ material thermal conductivity, $\rho =$ material density, $c_p =$ material specific heat capacity and $\omega =$ rotational speed of cylinder.

The following assumptions are implicitly made with the above:

- Conduction in the circumferential direction, occurring due phase differences in temperature fluctuations around the circumference, is assumed negligible compared to the radial direction.
- The change in conducting area due to cylindrical geometry is neglected
- The geometry is assumed infinite in the radial direction

Subsequent verification of these with regards to the conclusions drawn can be made from examining the solution and proposed design geometry.

Solving using separation of variables, with the calculated Fourier decomposition of the heat load, gives the following equation for the temperature fluctuations as a function of depth below the surface x and angular rotation $\theta = \omega.t$.

$$u(x,\theta) = Q0 \sum_{n} \frac{1}{\sqrt{k.\rho.c_p.n.\omega}} \cdot Re\left(C_n \cdot e^{i\left(n.\theta - \sqrt{n}.\frac{x}{\delta L} - \frac{\pi}{4}\right)}\right) \cdot e^{\left(-\sqrt{n}.\frac{x}{\delta L}\right)} \quad (3)$$

where C_n = Complex Fourier coefficients of flux ratio (Figure 4), dependant on orientation (ψ, β), $\delta L = \sqrt{\frac{2k}{\rho.c_p.\omega}}$ = spatial decay constant.

The temperatures are plotted in Figure 9 as a function of rotation angle for $x = 0$ and $x = \delta L$, for a rotational speed of 10 rev/s, Tungsten armour disc and nominal (reference plane) heat flux of 10MW/m2. Results are shown for zero and maximum azimuth angles, corresponding to the heat flux ratio plots in Figure 4. The maximum surface temperatures are plotted in Figure 10 as a function of the rotational speed. The temperature fluctuations decay exponentially and shift in phase from that of the surface. As the azimuth angle β is increased the surface temperatures are significantly reduced directly due to the lower heat flux ratio (Figure 4). For a static cylindrically profiled component, maximising β is essential to spread the heat load (as exploited in the topology optimisation covered in Section 0). To ensure the solution is robust however, maximising β must consider the sensitivity to operational plasma variability to ensure lower heat fluxes are maintained and shine-through is prevented. Although increasing β would also help with a rotating component, it is less essential as by rotating the component at a sufficient speed the lower temperatures can be maintained, even for $\beta = 0$, and providing a design that is robust to plasma variability and where shine-through is prevented.

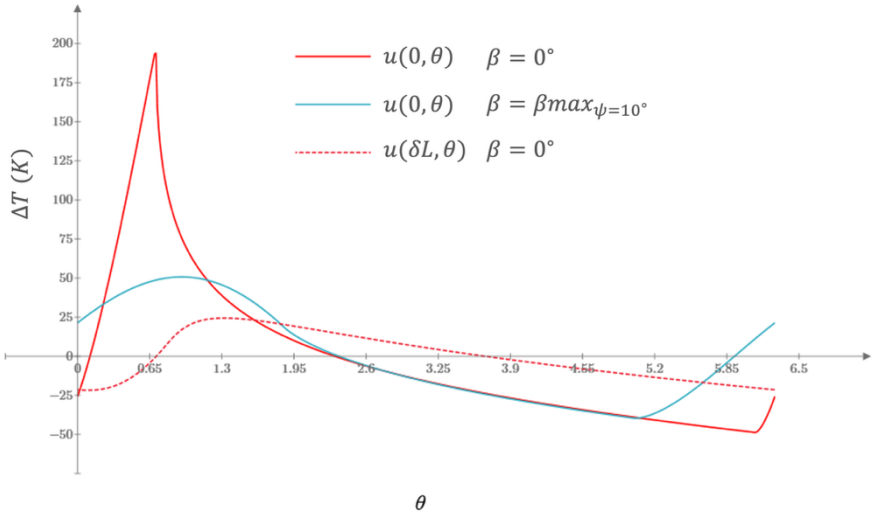


Figure 9. Temperature fluctuations at the surface ($x = 0$) and subsurface at $x = dL$, for a Tungsten disc with nominal heat flux of 10 MW/m2, $\omega = 10\ rev/s$, $\psi = 10\ deg$.

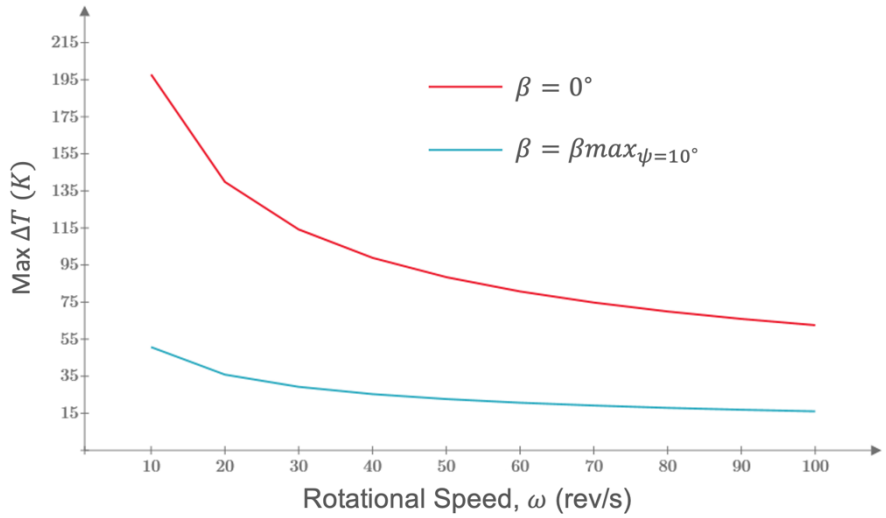


Figure 10. Maximum temperature change (from mean) as a function of rotational speed, $\psi = 10\ deg$.

The rate at which the temperatures decay below the surface is governed by the decay length δL and the harmonics of the loading (n). Lower harmonics and lower speeds penetrate deeper into the surface. Considering the lowest harmonic as the limiting case, Figure 11 plots the depth at which temperature fluctuations have decayed to 1% of that at the surface as a function of rotational speed for Tungsten. A rotational speed of 10 rev/s is sufficient to ensure temperatures have decayed to 1% at a depth of 5mm.

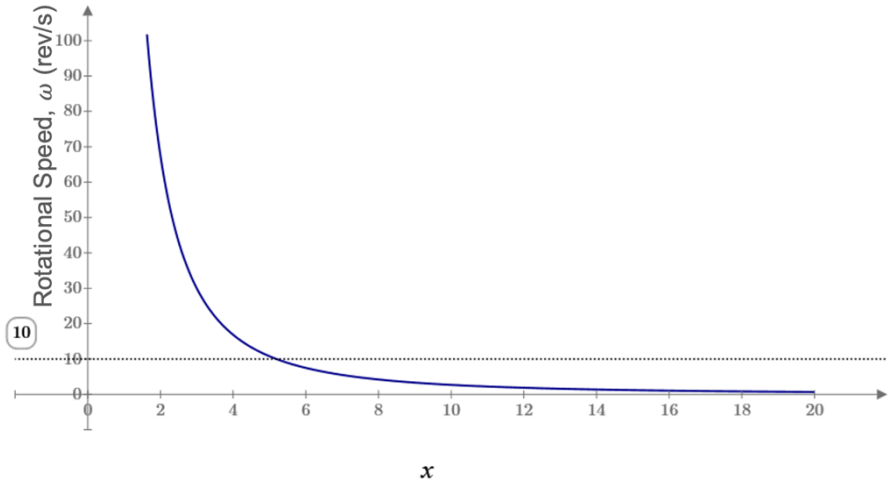


Figure 11. Rotational speed, ω to achieve temperature decay to 1% of surface value at depth x for (Tungsten).

5.2 Bearing Support and Overall Thermal – Structural Performance

The overall thermal performance of the design is dependent on the bearing support which effects the overall thermal resistance and ability to transfer the mean heat load (Equation 2). Two primary design options are considered, shown in Table 3 summarising the advantages, risks and issues.

Calculations were performed for a preliminary assessment of the potential for either option to provide improved thermal and structural performance based on the following assumptions:

- The rolling element (RE) bearing is assumed to provide complete structural isolation (stiffness is assumed negligible relative to disc and pipe)
- RE bearing dimensions are based on approximate dimensions from manufacturer data
- A material of Silicon Carbide is assumed for the raceway and balls for the RE bearing
- A RE bearing with acceptable performance / durability is assumed to be obtainable – must be confirmed through supplier engagement and further calculations
- A nominal clearance for the hydrodynamic bearing of $0.002 \times D$ is assumed
- The performance (operating minimum clearance) of the hydrodynamic bearing is assumed acceptable – must be confirmed by more detailed bearing performance calculations considering specific lubricant options

Temperatures were calculated by modelling the component as a series of thermal resistances as shown in the systems model in Figure 12.

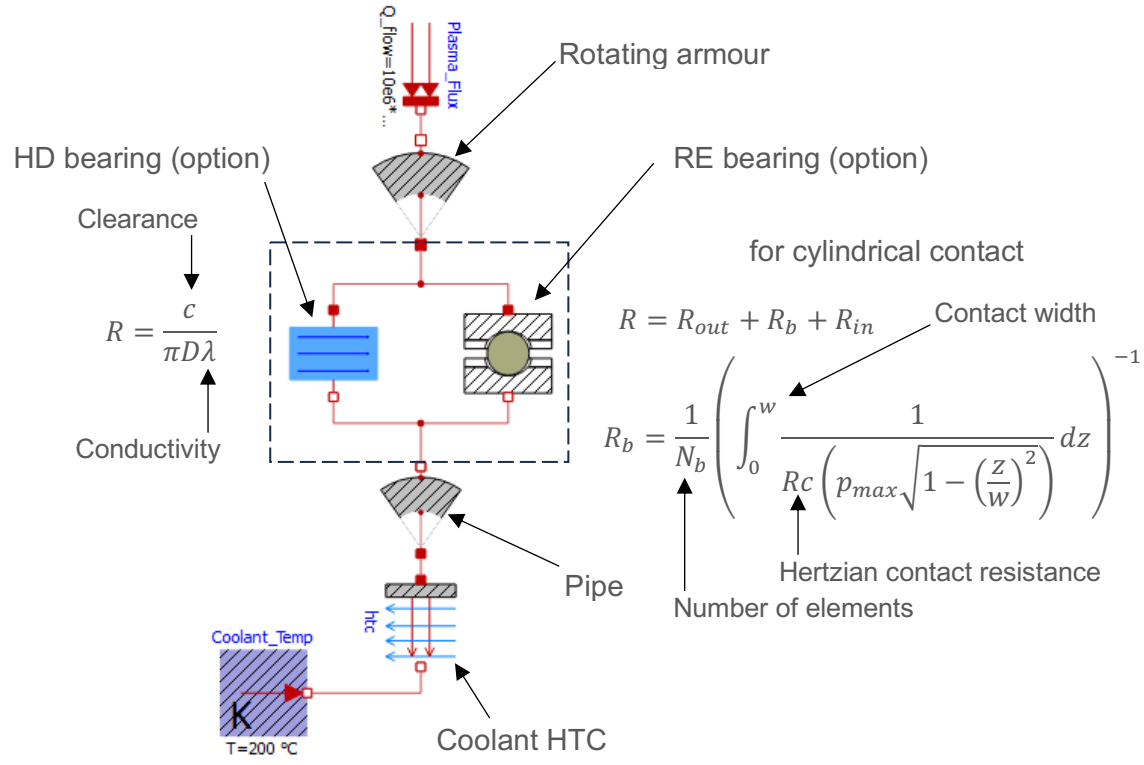
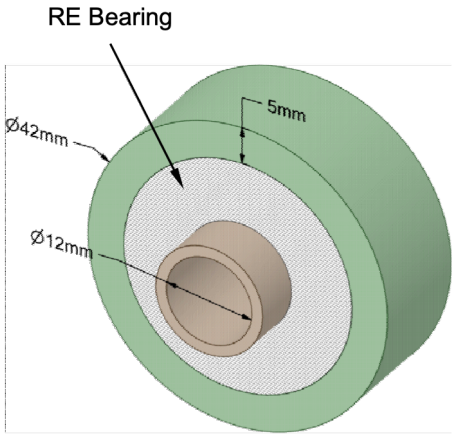
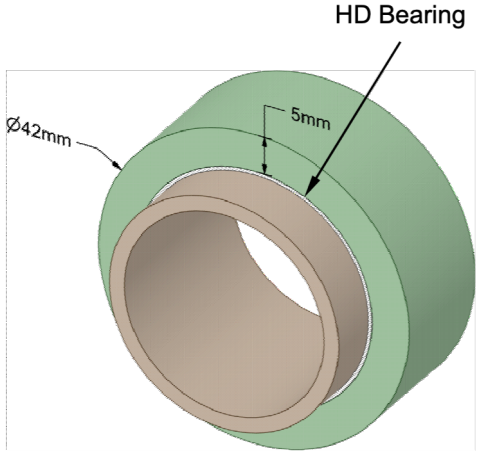


Figure 12. Thermal systems model in Modelica (using ARTEMIS-Core library).

Table 3. Bearing support design advantages, risks and issues summary.

Design	Advantages	Risks / Issues
Ultra-High-Vacuum (UHV) Rolling Element (RE) bearing 	No bearing lubrication required using lubricant free UHV bearing technology.	Thermal resistance across bearing (which is load dependant) must be sufficiently small to maintain acceptable temperatures within the PFC.
	Bearing compliance (relative to plasma facing disc) provides isolation between pipe and disc limiting issues due to differential thermal expansion.	Required load may not be achievable for the bearing size and lifetime.
		Pre-load must be retained under thermal expansion,
		Pre-load may adversely affect compliance.
		Compatibility of the bearing materials for Fusion power plant conditions.
Hydrodynamic (HD) bearing 	Full isolation between plasma facing disc and pipe	Thermal conductance is highly dependent on lubricant used and maintaining bearing clearance under operating conditions.
	Potential for better thermal conductance.	Compatibility and loss of lubricant into plasma. Potential use of labyrinth seals? Potential use of liquid metals?
		Lubricant supply – potential to combine with coolant but thereby limiting coolant choice

For the rolling element bearing the hertzian contact resistance was calculated using the Greenwood and Williamson model with Lambert-Fletcher correlation for asperity slope [10]. The total thermal resistance and resulting peak temperature at the plasma facing surface are dependent on the rolling element bearing load or hydrodynamic bearing lubricant conductivity for the designs respectively. The peak temperatures are therefore plotted in Figure 13 as a function of these parameters.

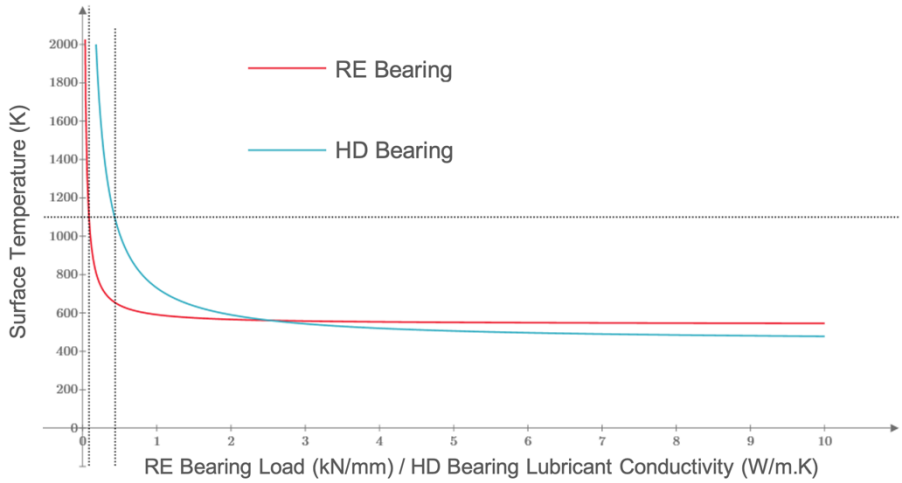


Figure 13. Peak surface temperature as a function of rolling element bearing load or hydrodynamic bearing lubricant conductivity.

The results show that to maintain the peak temperature to a similar value as with the reference Monoblock design (see Figure 7.a), under the same nominal reference plane heat flux of 10 MW/m2, a RE bearing load of ≈0.1 kN/mm or an HD bearing lubricant conductivity of ≈0.433 W/m.K (similar to water) is required. In practice any design advantage is best exploited through increasing the heat loading capacity within acceptable temperature and durability limits. Higher temperatures should be possible with the rotating PFC design due to reduced durability constraints from:

- removal of the need for an interlayer,
- structural isolation of the disc from the pipe,
- axisymmetric mean thermal loading.

Based on the assumptions stated previously stresses were calculated, in this case using the UKAEA ARTEMIS-Core Modelica library, with a thermally loaded axisymmetric cylinder under plane stress conditions.

Figure 14 instead plots the reference plane heat flux capacity relative to the baseline, as a function of the bearing variable, considering both a) limiting the peak temperatures to that of the baseline reference design and b) limiting the maximum stresses in the Tungsten to within yield.

As the bearing load or lubricant conductivity are increased the heat flux capacity asymptotically approaches a limiting value set by the fixed thermal resistances. This preliminary assessment shows a significant potential of the concept to handle much greater heat fluxes of up to over 2.5x that of the baseline reference design, providing sufficient RE bearing load or HD bearing lubricant conductivity can be obtained. Some lubricant conductivities are overlaid in Figure 14 for reference. The practical ability to achieve this however must be confirmed through further work to address the detailed aspects of the design and to ensure the operating assumptions made here are valid.

The surface fluctuations in temperature are, as shown previously, dependant on the achievable rotational speed. This will of course introduce some additional localised cyclic

stresses at the surface subject to many more cycles than that from repeated plasma pulses. Calculations on the magnitudes and consequence of these on fatigue is left to be performed alongside development of other aspects of the concept. These stresses will be compressive however and occur at the outer surface, also under a state of compressive stress from the main thermal cycle, and therefore the impact on durability is expected to be low.

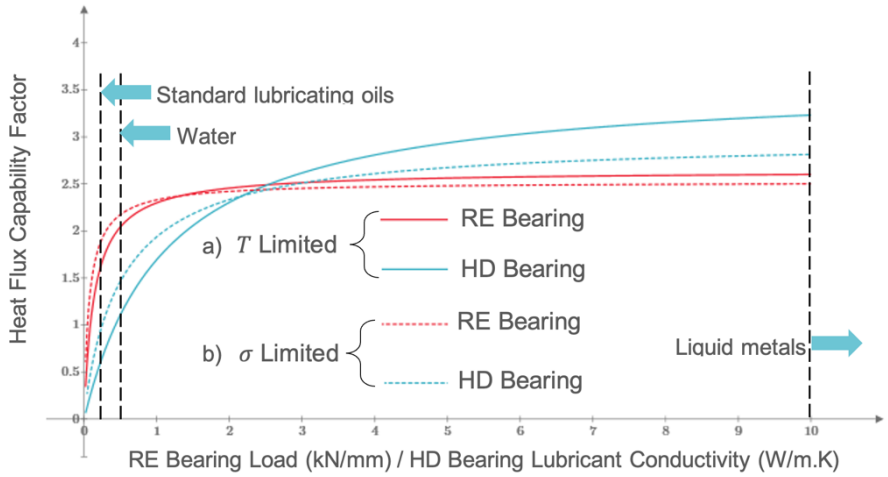


Figure 14. Heat flux capability as a function of RE bearing load or HD bearing lubricant conductivity.

5.3 Driving Rotation

There are two primary means of driving the rotation which can be considered. An active drive via a vacuum rotary feedthrough or a passive drive utilising the tokamak magnetic field and electrical currents which naturally flow through the structure. In either case it is important to note that precise control of the speed is not necessary providing a minimum speed can be maintained during plasma flat-top operation. Although the active drive is technically feasible it is likely to become quite complex in terms of a feedthrough which is compatible with the environment and transmitting this drive through to the individual plasma facing components. A brief assessment of the feasibility of the passive drive is outlined below.

Under various mechanisms the interaction of the plasma ions with the wall generates electrical currents which flow though the components and the connecting tokamak structure [11],[12],[13]. The dominant mechanism and nature of these currents is complex and dependant on the specific magnetic configuration of the device and operating scenario. In general, the electrical current flowing through the component combined with the local magnetic field will generate a Lorentz force density on the component as illustrated in Figure 15 for a point on the surface.

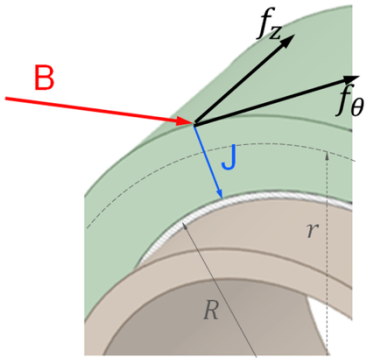


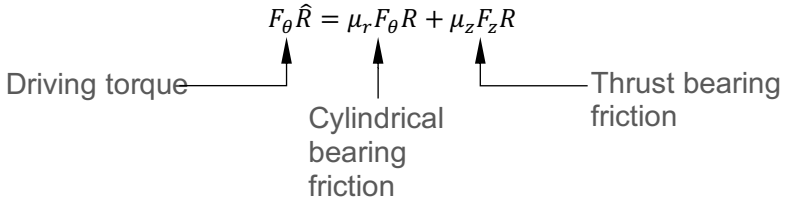
Figure 15. Field, current and Lorentz force vectors on component.

Integrating this and the moments of it about the rotational centre provide the net force to be reacted by the bearing and the driving torque respectively.

$$\bar{F} = \int_V \bar{J} \times \bar{B}$$

$$\bar{T} = F_\theta \hat{R} = \int_V r \cdot (\bar{J} \times \bar{B})$$

Equating the driving torque to the bearing frictional torque results in the following non-dimensional equation, where the effective friction coefficients μ_r, μ_z are functions of the respective bearing operating parameters.



$$\therefore \frac{\hat{R}}{R} = \mu_r + \mu_z . f(\beta, \psi) \tag{4}$$

For a preliminary feasibility assessment an HD bearing is considered and assuming the component is orientated to the magnetic field such that the axial (thrust) load is negligible ($F_z/F_\theta = f(\beta, \psi) \approx 0$). The friction coefficient μ_r, as well as the bearing Sommerfeld number (relating load and speed), can be formulated as a function of the operating eccentricity [14]. Assuming a short aspect ratio these are given by equations (5) and (6) below, also assuming the operating eccentricity is small ($\epsilon \ll 1$) which can be subsequently confirmed.

$$\varepsilon = \frac{4\pi}{\mu_r} \left(\frac{D}{L}\right)^2 \frac{c}{R} \tag{5}$$

$$S = \frac{L.D.\eta.N}{F_\theta} \left(\frac{R}{c}\right)^2 = \left(\frac{D}{L}\right)^2 \frac{4}{\varepsilon} \tag{6}$$

where, $D = 2R =$ bearing diameter, $c =$ bearing radial clearance, $L =$ bearing length, $\eta =$ fluid viscosity and $N =$ rotational speed of cylinder (rev/s).

Along with equation (4) these can be solved to relate the applied load to the steady state operating eccentricity and speed. Combining these equations and for the purpose of a feasibility assessment, assuming the field and current to be constant through the cylinder thickness, allows an explicit equation to be defined relating the current to the rotational speed.

$$Ic = \frac{\pi.L.D.\eta.N}{B.t} \left(\frac{R}{c}\right) \left(\frac{R}{\hat{R}}\right)$$

Taking some approximate geometric values ($L = 10mm,\ R = 16mm,\ t = 5mm,\ \therefore \hat{R} = R + t/2 = 18.5mm,\ c = 0.002D$), a bearing viscosity of the order of that of liquid metals $\eta = 2.mPa.s$, and a local magnetic field of the order of $3T$, gives a required current of $\approx 2.9A$ to rotate at 10 rev/s. Although a number of assumptions are made here this shows the electrical current required to rotate the cylinder at the necessary speed should be practically feasible.

5.4 Challenges

The calculations above have shown a potential for increased heat flux capacity in a novel design to rotate the plasma facing component. How much of the potential benefit can be

realised in practice is dependent on remaining challenges being investigated further along with appropriate supporting calculations. These include:

- More detailed consideration of the electrical current flows and consequence on the passive drive maintaining a sufficient rotational speed, in conjunction with the bearing design.
- The risks and issues summarised in Table 3 associated with the operational performance (lifetime, compatibility, manufacturability, etc.) of the bearing arrangement.
  - RE bearing pre-load, compatibility and lifetime in power plant power environment.
  - HD bearing lubricant compatibility, supply, sealing and loss rate.
- Cost of design - likely to be high for RE bearing.

Prior to further study on this concept, the most promising in terms of complexity and cost is likely to be in the use of a hydrodynamic bearing, using a form of labyrinth seal to minimise the lubricant loss. Combination of this concept with other proposed liquid metal armour concepts [5], using the high conductivity liquid metal as the bearing lubricant, is also worth consideration.

6 Conclusions

This paper has applied specific analysis techniques to rapidly investigate potential adaptions to the Monoblock plasma facing component architecture of a fusion power plant. In doing so this has also demonstrated the freedom that utilisation of these appropriately simplified techniques provides to investigate potential designs at an early concept stage.

The results have shown significant potential in topology optimisation of the armour structure, combined with shape optimisation of the plasma facing surface to reduce the Tungsten requirement by close to 60% whilst maintaining similar thermal-structural performance. This design has potential for significant savings in material costs within the current heat loading operating envelope.

Separately, with an aim to improve the heat loading capacity by more optimal use of the armour material and coolant convection surface, a novel solution was proposed using rotation of the component to distribute the heat flux. Results showed a potential in this concept to significantly improve the heat loading capacity by a factor of up to 2.5.

In both cases further work and analysis are needed to address the remaining challenges to quantify the design risk and resulting likelihood of being able to realise the potential benefits outlined.

7 Acknowledgement

This work has been funded by STEP Fusion, a major technology and infrastructure programme led by UK Fusion Energy Ltd (UKFE), which aims to deliver the UK’s prototype fusion powerplant and a path to the commercial viability of fusion.

8 References

[1] A. Hassanein, “Prediction of material erosion and lifetime during major plasma instabilities in tokamak devices,” Fusion Engineering and Design, vol. 60, no. 4, pp. 527–546, Jul. 2002, doi: 10.1016/S0920-3796(02)00008-X.

[2] S. Ratynskaia et al., “Runaway electron-induced plasma facing component damage in tokamaks,” Plasma Phys. Control. Fusion, Nov. 2025, doi: 10.1088/1361-6587/ae1c6c.

[3] Ch. Linsmeier et al., “Development of advanced high heat flux and plasma-facing materials,” Nucl. Fusion, vol. 57, no. 9, p. 092007, Sep. 2017, doi: 10.1088/1741-4326/aa6f71.

[4] C. S. Wiggins, A. Cabral, and L. B. Carasik, “Heat Transfer Performance of Cu-Cr-Zr Tube with Swirl Insert Under Cyclic Thermal Loading in Monoblock Divertor,” Fusion Science and Technology, vol. 77, no. 7–8, pp. 710–715, Nov. 2021, doi: 10.1080/15361055.2021.1898304.

[5] J. S. Hu et al., “Recent progress in the development of liquid metal plasma facing components for magnetic fusion devices,” Nuclear Materials and Energy, vol. 41, p. 101776, Dec. 2024, doi: 10.1016/j.nme.2024.101776.

[6] R. A. Pitts et al., “Physics conclusions in support of ITER W divertor monoblock shaping,” Nuclear Materials and Energy, vol. 12, pp. 60–74, Aug. 2017, doi: 10.1016/j.nme.2017.03.005.

[7] M. P. Bendsøe and O. Sigmund, Topology Optimization. Berlin, Heidelberg: Springer Berlin Heidelberg, 2004. doi: 10.1007/978-3-662-05086-6.

[8] G. Allaire, F. Jouve, and A.-M. Toader, “Structural optimization using sensitivity analysis and a level-set method,” Journal of Computational Physics, vol. 194, no. 1, pp. 363–393, Feb. 2004, doi: 10.1016/j.jcp.2003.09.032.

[9] T. R. Barrett et al., “Virtual Engineering of a Fusion Reactor: Application to Divertor Design, Manufacture, and Testing,” IEEE Trans. Plasma Sci., vol. 47, no. 1, pp. 889–896, Jan. 2019, doi: 10.1109/TPS.2018.2856888.

[10] M. A. Lambert and L. S. Fletcher, “Review of Models for Thermal Contact Conductance of Metals,” Journal of Thermophysics and Heat Transfer, vol. 11, no. 2, pp. 129–140, Apr. 1997, doi: 10.2514/2.6221.

[11] M. J. Schaffer and B. J. Leikind, “Observation of electric currents in diverted tokamak scrape-off layers,” Nucl. Fusion, vol. 31, no. 9, pp. 1750–1758, Sep. 1991, doi: 10.1088/0029-5515/31/9/013.

[12] Staebler, G. M., and F. L. Hinton. “Currents in the Scrape-off Layer of Diverted Tokamaks.” Nuclear Fusion, vol. 29, no. 10, Oct. 1989, pp. 1820–24. DOI.org (Crossref), https://doi.org/10.1088/0029-5515/29/10/017.

[13] Rozhansky, V., et al. “Currents Structure in the Scrape-off Layer of a Tokamak.” *Nuclear Materials and Energy*, vol. 25, Dec. 2020, p. 100840. *DOI.org (Crossref)*, https://doi.org/10.1016/j.nme.2020.100840.

[14] R. Gohar, H, Rahnejat. (2008). “Fundamentals of Tribology”. Imperial College Press.